2014-01-1606
Published 04/01/2014

doi:10.4271/2014-01-1606
saefuel.saejournals.org

Novel Characterization of GDI Engine Exhaust for Gasoline and Mid-Level Gasoline-Alcohol Blends

John M. Storey, Sam Lewis, James Szybist, John Thomas, Teresa Barone, Mary Eibl, Eric Nafziger, and Brian Kaul
Oak Ridge National Laboratory

ABSTRACT

Gasoline direct injection (GDI) engines can offer improved fuel economy and higher performance over their port fuel-injected (PFI) counterparts, and are now appearing in increasingly more U.S. and European vehicles. Small displacement, turbocharged GDI engines are replacing large displacement engines, particularly in light-duty trucks and sport utility vehicles, in order for manufacturers to meet more stringent fuel economy standards. GDI engines typically emit the most particulate matter (PM) during periods of rich operation such as start-up and acceleration, and emissions of air toxics are also more likely during this condition. A 2.0 L GDI engine was operated at lambda of 0.91 at typical loads for acceleration (2600 rpm, 8 bar BMEP) on three different fuels; an 87 anti-knock index (AKI) gasoline (E0), 30% ethanol blended with the 87 AKI fuel (E30), and 48% isobutanol blended with the 87 AKI fuel. E30 was chosen to maximize octane enhancement while minimizing ethanol-blend level and iBu48 was chosen to match the same fuel oxygen level as E30. Particle size and number, organic carbon and elemental carbon (OC/EC), soot HC speciation, and aldehydes and ketones were all analyzed during the experiment. A new method for soot HC speciation is introduced using a direct, thermal desorption/pyrolysis inlet for the gas chromatograph (GC). Results showed high levels of aromatic compounds were present in the PM, including downstream of the catalyst, and the aldehydes were dominated by the alcohol blending.

CITATION: Storey, J., Lewis, S., Szybist, J., Thomas, J. et al., "Novel Characterization of GDI Engine Exhaust for Gasoline and Mid-Level Gasoline-Alcohol Blends," *SAE Int. J. Fuels Lubr.* 7(2):2014, doi:10.4271/2014-01-1606.

INTRODUCTION

Light-duty vehicles with direct injection gasoline (GDI) engines have been in commercial production since the late 1990's [1],[2], but have only become common in the U.S fleet in the past four years. Most manufacturers offer several passenger car and light-duty truck/SUV models with GDI engines, and it is widely accepted that smaller displacement, turbocharged GDI engines will replace larger displacement engines as one means for manufacturers to meet higher light-duty vehicle fuel economy regulations. Turbocharged GDI engines can be more fuel efficient and also offer a performance benefit due to the higher volumetric efficiency at high load [3]. However, GDI engines tend to produce more PM than their port fuel-injected (PFI) counterparts [4],[5],[6],[7],[8],[9], with PM mass levels exceeding those of diesels equipped with diesel particulate filters, as well as conventional port-fuel injected vehicles [10],[4],[11]. Because of the impact of mobile sources on air quality, any large-scale change in engine technology and fuel may have far-reaching effects. As ambient air standards for fine PM decrease, direct emissions of PM from GDI vehicles may affect the air quality attainment status of regions.

With the passage of the Energy Independence and Security Act (EISA 2007), the U.S. Congress set specific goals for the use of renewable fuels (36 billion gallons by 2022). The majority of this goal is expected to be met with ethanol from both corn and “advanced biofuel” sources like cellulosic feedstocks. The mandated volume of ethanol is likely to be utilized as fuel for flex-fuel vehicles (E51-E83) and as other blending components of gasoline higher than the current 10% level. In 2010 and 2011, the U.S. EPA granted a partial waiver for the use of E15, 15% ethanol, in model year 2001 and later gasoline vehicles [12]. Furthermore, E30 has been identified as a potential high octane rating fuel that will enable fuel efficient technologies such as low-speed and high boost without end-gas knock concerns [13]. Beyond ethanol, butanol is also gaining momentum as a renewable fuel. Butanol can be made in similar production facilities to ethanol and its vapor pressure and energy density more closely match gasoline.

Thus, there continues to be interest in seeing the effects of the convergence of two current technologies, GDI and alcohol fuel blends, on emission levels of PM and other pollutants. Our laboratory and others have been investigating ethanol blend effects on in-use gasoline vehicles and PM emissions [5],[8],[7],[14],[6]. In this paper, the emissions of a GDI engine

fueled with gasoline (E0), 30% ethanol in gasoline (E30) and 48% isobutanol in gasoline (iBu48) are characterized. (The iBu48 is not envisioned as a future fuel, but was selected to match the oxygen content of the E30 blend). A novel method for characterizing soot hydrocarbons (HCs) is presented, and the emissions differences relative to the alcohol blends are illustrated.

EXPERIMENTAL METHODS

Engine Specifications and Operating Conditions

The engine used in this study has been specifically developed for high-efficiency operation with ethanol [15]. The engine is a modified four-cylinder 2.0 L GM direct-injection spark-ignition (DISI) engine with turbocharging, dual independent cam phasing, and a 2-step valve train that enables both early and late intake valve closing for unthrottled operation for most of the load range. This study uses the high lift late intake valve closing strategy. The engine was equipped with a factory three-way catalyst. Engine geometry and specifications are provided in Table 1. A description of the unique engine hardware, control, and data acquisition can be found in Szybist et al. [14].

Throughout the experiment the engine was operated at an engine speed of 2600 rpm and a load of 8 bar brake mean effective pressure (BMEP) under rich conditions (λ=0.91). Fuel rail pressure was held at a constant 85 bar with a constant start of injection timing of 323-329 degrees of crank angle before top dead center (CA bTDC). Fuel injection duration was adjusted for each fuel to maintain load. Combustion phasing was also maintained constant by varying the spark timing from 15 to 17 degrees bTDC. Typical of an acceleration condition, this relatively high BMEP operating condition was of interest for soot production, because, as part of this research effort, we are investigating the soot oxidation properties of GDI soot. The soot oxidation studies require the collection of gram quantities of soot on gasoline particulate filter (GPF) substrates, necessitating long periods of operation at a high soot concentration [16].

To determine this particular operating condition, the A/F and soot levels during various load transients on a similar 2.0 L GM LNF engine with a transient-capable OEM controller were measured for several engine speeds. Figure 1 shows results from a transient test at 2600 rpm, in which the throttle position was changed from 30 to 60%. Soot concentration was measured with an AVL Microsoot sensor. The A/F ratio for steady-state testing was selected to be slightly higher than the minimum λ value of 0.89 from these tests due to operational temperature concerns. Note that the temporal response of the Microsoot sensor is 1 s so the signal is considerably broader than the lambda measurement.

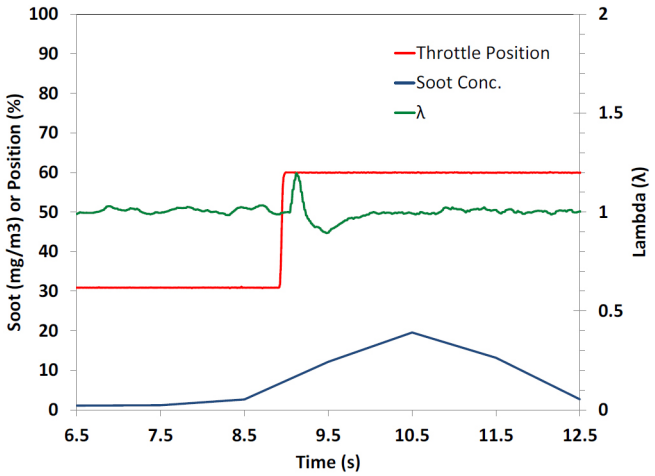

Figure 1. Transient response of A/F to step changes in throttle position. The photoacoustic soot sensor signal is superimposed at the bottom of the graph.

The speed-load combination that produced the highest soot concentration with the lowest temperature was selected for steady-state experiments. Low temperature is important to avoid auto-oxidizing the soot collected in the GPF cores during exposure. Steady-state operation at the selected speed-load point does not produce as high a particle concentration as shown in Figure 1, although the A/F ratio is the same. A steady-state soot concentration level of ~5 mg/m^3 was observed in the preliminary experiments, compared to the spike of approximately 20 mg/m^3 for the transient case shown.

Figure 2 is a schematic of the entire experimental system used to expose the GPF cores along with analytical techniques.

Table 1. Engine Geometry and Specifications

Displacement (L)	2.0
Bore (nm)	86
Stroke (nm)	86
Compression Ratio	11.85
Fueling	DI
DI Pressure (bar)	100

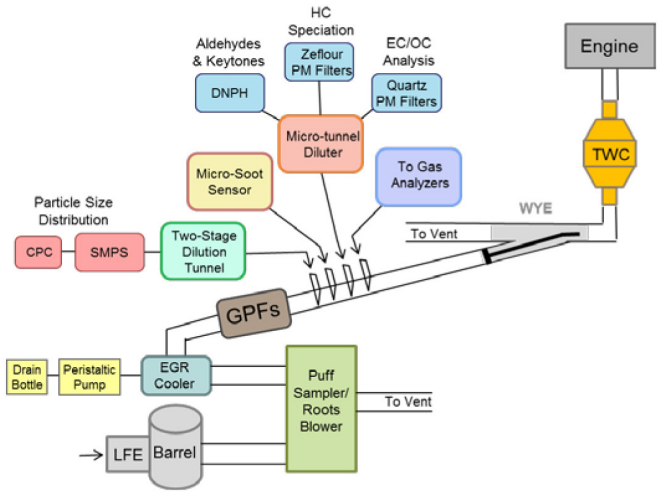

Figure 2. Schematic of experimental setup. Note that all exhaust PM measurements were conducted downstream of the three-way catalyst (TWC).

Fuels

The three fuels investigated in this study were an 87 anti-knock index (AKI) gasoline (E0), a 30% ethanol blend with 87 AKI gasoline (E30), and a 48% isobutanol blend with AKI gasoline (iBu48). E30 was chosen to maximize octane enhancement while minimizing ethanol-blend level and iBu48 was chosen to match the same fuel oxygen level as E30. Fuel properties are given in Table 2. While it is recognized by the authors that iBu48 would likely never be a marketplace fuel, it was felt that the GDI soot oxidation study would benefit from having soot generated with gasoline-alcohol blends having the same fuel oxygen level since that has proved to be an important parameter in past studies of biodiesel blend soot oxidation [16].

Also, it was thought that the enhanced fuel oxygen would amplify effects on the PM chemistry that might be too subtle with lower blends.

Table 2. Fuel Properties.

Fuel Property	ASTM Method:	E0	E30	iBu48
Alcohol (vol-%)		0	30.7	48
DVPE (kPa)	D5191	90.5	91.6	< 85
LHV (MJ/kg)	D240	43.4	38.1	39.7
SG (kg/l)	D4052	.0.729	0.745	0.76
C (wt-%)	D5291	86.0	74.8	75.3
H (wt-%)	D5291	14.0	13.9	13.8
O (wt-%)	D5599	0	11.3	10.9
Total Aromatics (wt-%)	D5580			
Sulfur (ppm)	D5453	6	12	14
Research Octane (RON)	D2699	90.2	100	>100
Motor Octane (MON)	D2700	83.9	88	>88

Sampling and Dilution Systems

Separate systems were used to condition post-three way catalyst exhaust for various particulate matter (PM) measurements:

1. A single-stage micro-tunnel dilution system to provide single dilution exhaust for particulate matter (PM) and DNPH cartridges; and
2. A two-stage dilution system to provide either single or double diluted exhaust to a Scanning Mobility Particle Sizer (SMPS).

The single-stage micro-tunnel dilution system is based on an ejector pump design by Abdul-Khalek et al. [17] in which raw exhaust is drawn into the dilution tunnel as dry, filtered, and compressed air is passed through an ejector pump. A critical orifice ahead of the ejector pump maintained a constant exhaust sample flow resulting in a dilution of 9-9.2. Following equipment warm up, a volumetric flow meter (DryCal DC-Lite) was used to measure the flow of High Efficiency Particulate Air (HEPA) filtered air. The dilution ratio was calculated as per Equation (1).

$$DR = \frac{\dot{m}_{air} + \dot{m}_{exhaust}}{\dot{m}_{exhaust}} \quad (1)$$

A stainless steel heated line fitted with a sampling probe supplied exhaust to the micro-diluter. The stainless steel line was heated to 190°C to reduce thermophoretic deposition of solid particles and condensation of volatile materials onto the wall of the sampling line. The diluted sample temperature was maintained at 40°C.

The two-stage dilution system is based on an ejector pump design similar to that of the European Particle Measurement Programme (PMP) [18]. This design consists of a micro-tunnel dilution system paired with an evaporator tube. In this system, air heated to 150°C flows in through an ejector pump pulling the exhaust sample through a 150°C first-stage dilution tunnel. The diluted sample is then drawn by a second ejector pump through a 350°C evaporator tube. Following a residence time of approximately 150 ms in the evaporator tube, the exhaust is further diluted with ambient temperature air as the sample enters the second-stage dilution. The second-stage dilution tunnel was maintained at 50°C, as required by the PMP. The dilution ratio for the two-stage dilution system was determined by a CO_2 ratio. The raw exhaust gas CO_2 (wet concentration) was determined and divided by the tunnel CO_2 concentration. The second stage dilution ratio was determined to be about 40. A short (< 0.3 m) length of insulated stainless steel tubing was used to deliver exhaust to the two-stage dilution system from the exhaust pipe.

Two test procedures were performed to validate proper operation of the ORNL two stage dilution system design. First, an aerosolized sodium chloride solution was passed through the dilution system to confirm a zero net loss of solid particulate between first-stage and second-stage dilution. Second, a calibration procedure similar to that of UN-ECE Regulation 83 was performed [19]. For this procedure volatile tetracontane (C40) particles produced by an aerosol generator were sampled through the two stage dilution system. The polydisperse C40 particles were detected by the SMPS after first stage dilution at an approximate concentration of $3.8 \times 10^3/cm^3$. Near complete vaporization of the volatile particles was observed after second stage dilution. The volatile particle removal efficiency was determined to be >99% for the two stage dilution system.

PM SAMPLING AND ANALYSIS

PM Mass

Succeeding dilution by the micro-tunnel dilution system PM samples were collected for soot HC speciation analysis. The PM samples were collected on 70mm filters cut from 20×25 cm sheets of PTFE membrane filter paper (Zefluor™, Pall Corp.). Filters were conditioned and weighed in an environmentally controlled chamber (Model 518, ETS Inc.) prior to and following filter loading with a 1 µg sensitivity Sartorious balance. Due to the amount of PM required for analysis, large sample volumes were used. Filter volumes for the E0, E30, and iBu48 fuels were 5664, 11134, and 7772 L respectively, resulting in filter PM masses of 3.6 - 6.2 mg.

PM Hydrocarbon Speciation Technique

A novel sampling and analytical methodology was developed specifically to achieve direct analysis of the organic hydrocarbon compounds from the PM filter samples. This approach used a combination of gentle vacuum suction to harvest PM from the filter surface without the need for solvent extraction and its attendant risks of biasing, volatiles-loss, and contamination. The supported membrane filters can tolerate suction, unlike the thin membrane types, e.g. Teflon®. There is also is no loss of mass, which could happen with a fiber filter like a PTFE-coated glass fiber filter. Experiments with blank filters showed no weight loss after undergoing the suction procedure. After being vacuum harvested, the PM was loaded into the sample vessel shown in Figure 1 and subsequently underwent analysis by thermal desorption/pyrolysis gas chromatography mass spectrometry (TDP-GC-MS) using a multi-shot pyrolysis injector (Frontier Laboratories, Ltd model EGA/PY-3030D) coupled to a GC-MS (Agilent 5975). The TDP-GC-MS is well suited to GDI PM analysis because small amounts of PM (< 1 mg) are collected and directly analyzed. Typical solvent extraction methods suffer from bias due to the efficient extraction of compounds of a polarity that matches the solvent, but less efficient extraction of compounds that differ in polarity.

In the development of a single-shot thermal analysis of a soot sample, a comparison study was completed using subsamples from four 1 mg soot samples collected from a surrogate EGR cooler tube. Two of the samples were extracted with acetone-hexane solvent using a microwave-enhanced technique described previously. The solvent-extracted samples were analyzed by a direct injection method. The method included a 2 µl injection made in splitless mode and separated using a capillary column (Restek RXi-5MS 30m, 350 µm id, 0.25 µm film). The GC's temperature program started from an initial temperature of 40 °C for 3 min then ramped from 40-320 °C at 6 °C per min and held at 320 °C for 5 min. The compounds were analyzed by MS, which was scanned from 35 to 550 daltons at a 1 s scan rate. The TDP-GC-MS allows the smaller more volatile compounds to be thermally removed from the soot and analyzed before the matrix compounds are removed and analyzed thus reducing the complexity of the analysis. Also, the solvent free extraction of organic compounds from soot shortens the total analysis time and cost. For this study, the thermal analysis of the soot sample was conducted by purging the sample with helium for 30 sec then thermally desorbing it at 300 °C. The desorbed compounds were then transferred into the GC-MS and analyzed using the same GC-MS conditions as described above. Figure 2 shows chromatograms resulting from the two methods, scaled for injection amount. The direct method delivered more of the oxygenated compounds onto the column because there were no differences in solubility.

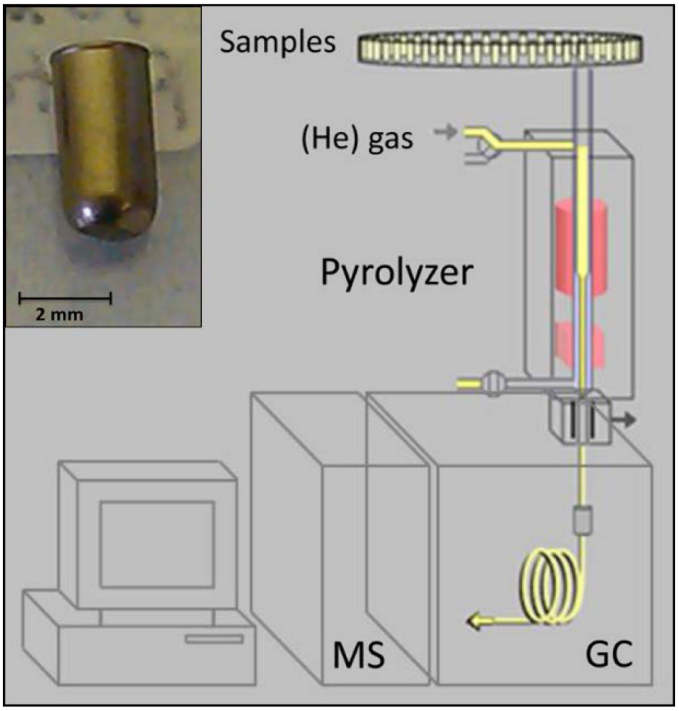

Figure 3. TDP-GC-MS schematic with inset image of sample vessel.

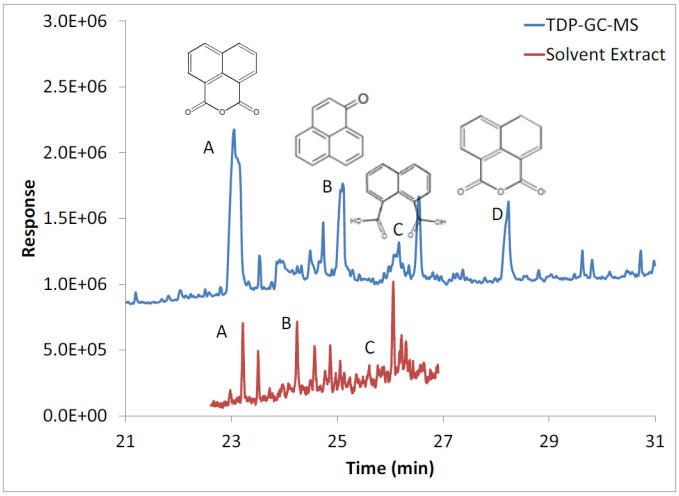

Figure 4. A comparison of chromatograms for solvent extract from 1 mg of soot and the direct thermal desorption of 1 mg of the same soot. Note that the signal-to-noise ratio is about 10x higher for the thermal desorbed sample and that compound D is not illustrated on the solvent extract sample. Compounds are typical oxygenated polycyclic aromatic hydrocarbons that are difficult to remove. A= 1,8 naphthalenic anhydride; B= 1-H phenalen-1-one; C = 2, 3 naphthalenedicarboxylic acid; D = 3-hydro-1, 8 naphthalenic anhydride.

In the current study, the conditions were largely the same except the first stage desorption was ramped to 325 °C. Also, a second pyrolysis step was performed on the same sample. After completion of the first GC-MS run for the thermally-desorbed compounds, the thimble is immediately heated to 500 °C under helium. This results in the breakdown of the soot matrix, potentially illustrating differences in the soot formation process. As will be described below, the second pyrolysis step also resulted in further recovery of the most non-volatile species.

PM Size and Number Concentration

An SMPS (Model 3936, TSI Inc.) equipped with the differential mobility analyzer (DMA, Model 3085, TSI, Inc.) and condensation particle counter (CPC, Model 3025, TSI, Inc.) was used for particle number concentration and number size distribution measurements. The two-stage dilution system was used to supply dilute exhaust to the SMPS. Number-size distributions were measured for particles 6 to 200 nm.

OC and EC Sampling

For analysis of elemental and organic carbon content of DISI PM, single dilution exhaust from the micro-tunnel diluter was filtered through pre-fired 47 mm quartz filters (QAOT2500-UP, Pall Corp.). The filters were analyzed by Sunset Laboratory Inc. (Tigard, OR) using the NIOSH 5040 thermo-optical transmission method [20]. For each sample a primary and secondary filter was used. The OC value of the secondary filter is subtracted from the primary filter OC value in order to correct for filter gaseous absorption artifacts, under the assumption that, at steady state, the amount of gaseous HCs that adsorb to the quartz filter media is the same for the primary and secondary filters, and thus the difference represents the OC fraction of the PM.

ALDEHYDE SAMPLING AND ANALYSIS

Gaseous aldehydes and keytones were collected using di-nitrophenyl hydrazine (DNPH)-coated solid phase extraction cartridges (Waters Corp.). The sample flow rate was 1.0 liter/min. A minimum of two DNPH cartridges were collected for each fuel type. Directly following sample collection, DNPH derivatives were solvent extracted with acetonitrile. Determination of aldehyde and keytone concentrations was performed by a Hewlett-Packard 1100 high performance liquid chromatograph (HPLC) using a Restek Allure C18 column with ultraviolet absorption detection. The eluent of the HPLC unit was transferred directly to a Bruker Daltonics® Esquire mass spectrometer where the hydrazone derivatives were positively identified using electrospray with negative ionization mass spectrometry (ESI-MS).

RESULTS

The results of the PM mass sampling are shown in Table 3. Note that the iBu48 and E0 have similar mass concentrations, but E30 shows a reduction in mass, consistent with earlier studies with E20 [6].

Table 3. PM mass sampling results

	E0	E30	iBu48
PM Mass (mg)	3.512	6.272	4.642
Exhaust Sampled (L)	5664	11134	7772
Dilution Ratio	9.1	9.0	9.2
Soot Raw (mg/m3)	5.62	5.07	5.50

The organic carbon and elemental carbon results are shown in Figure 5, with IB48 representing the results for the iBu48 fuel. The data were highly variable for OC, most likely for two reasons: 1) based on visual observation of filters, the sampling times were short (< 5 min) to prevent the accumulation of too much carbon. This short sampling interval may have resulted in a non-equilibrium condition for the gaseous HC, and thus variability; 2) in general, GDI PM is ~90% EC, so small changes in OC can lead to variability. Based on these data, the PM was 43%, 85%, and 95% EC for E0, E30, and iBu48, respectively. The higher OC content for E0 is consistent with the GC-MS results of the PM shown in Figure 6.

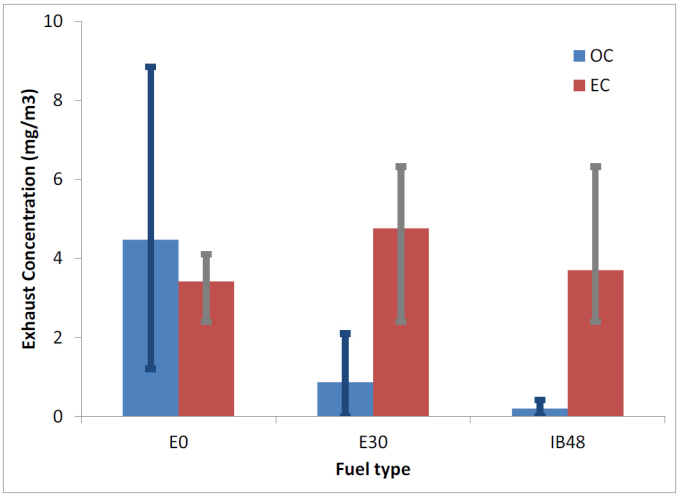

Figure 5. Average organic carbon (OC) and elemental carbon (EC) content of the exhaust PM for three fuels. Range bars show the maximum and minimum values.

PM Hydrocarbon Speciation Results

The PM from each of the three fuels was subjected to a two-step thermal desorption/pyrolysis process as detailed previously. A GC-MS chromatogram is shown in Figure 6. Note that the results for the iBu48 fuel are designated IB48 in Figures 6, 7, 8, 9, 10. Each organic species in Figure 6 is

represented by a peak on the trace, and the height and area of the response is proportional to the amount of the organic material in the sample. The traces are offset vertically for clarity. The response values have been normalized in two ways: the first was to the mass of soot desorbed, and the second was to the volume percentage of gasoline in the fuel. Thus, the mass-normalized values for E30 and iBu48 were divided by 0.7 and 0.52, respectively, to remove any "fuel dilution effects." Despite this adjustment, Figure 4 shows clearly that the E0 PM has richer chemistry and higher amounts of individual species. The exception is the peak at 26.6 min, pyrene, the amount of which is higher for the iBu48.

Of particular interest to this study are the high relative amounts of PAHs. Earlier speciation of diesel soot in this laboratory identified fewer PAHs, and those PAHs tended to be far less abundant than fuel species such as normal and branched alkanes. The lack of fuel species in gasoline exhaust PM is not unexpected due to the higher volatility, but the rich variety of PAHs is very different than for diesel soot.

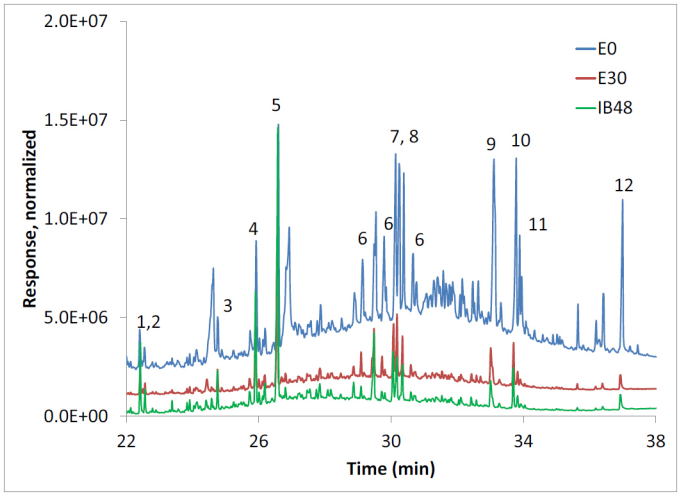

Figure 6. GC-MS trace of soot thermal desorption, showing a variety of PAHs. 1,2=phenanthrene, anthracene, 3=phenylnphthalene, 4=fluoranthene,5=pyrene, 6=various 4-ring PAH-ketones, 7,8= benz(a) anthracene, 8=chrysene, 9=benzofluoranthene, 10=benzo(a)pyrene, 11= benzo(e)pyrene, 12 = benzo(g,h,i)perylene.

Pyrolysis of the same soot samples was performed after the thermal desorption and the results are shown in Figures 7 and 8. Figure 7 shows a similar region of the chromatogram as Figure 6, and illustrates that additional amounts of the 5, 6, and even 7 ring PAHs are removed during the pyrolysis step, although in small amounts relative to Figure 6. Coronene, the compound whose structure is illustrated on Figure 7, has a very high boiling point and is likely to require the high temperatures of the pyrolysis step to be removed.

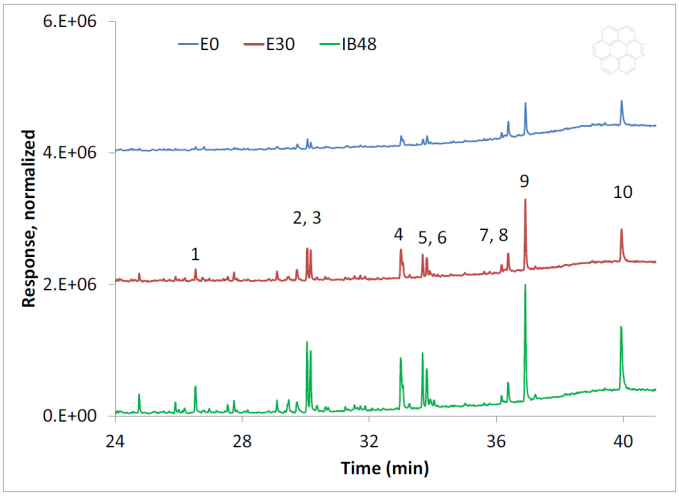

Figure 6. GC-MS of soot pyrolysis, showing the multi-ring PAH region. 1=pyrene, 2,3=benz(a)anthracene, chrysene, 4=benzofluoranthene, 5,6=benzo(a,e)pyrene, 7,8=indeno(1,2,3-cd)pyrene, dibenzo(a,h) anthracene, 9=benzo(g,h,i)perylene, 10=coronene (structure shown)

Figure 8 shows a separate region of the chromatogram, the front end, where the building blocks of the soot matrix elute after pyrolysis. Unlike the heavy PAHs shown in Figure 7, these compounds are light monoaromatics. Note that the prior temperature history of the soot sample was much too high for these compounds to be present as adsorbed molecules, so their source of these molecules is the breakdown of the soot matrix itself. Benzene, toluene, and styrene can be expected to form the major structural components of soot. Of interest is the presence of methyl propenoate for the E30 sample that is not present in the E0 or iBu48. Methyl propenoate is an unsaturated ester and thus may represent a portion of the soot structure that incorporated fuel oxygen into the backbone.

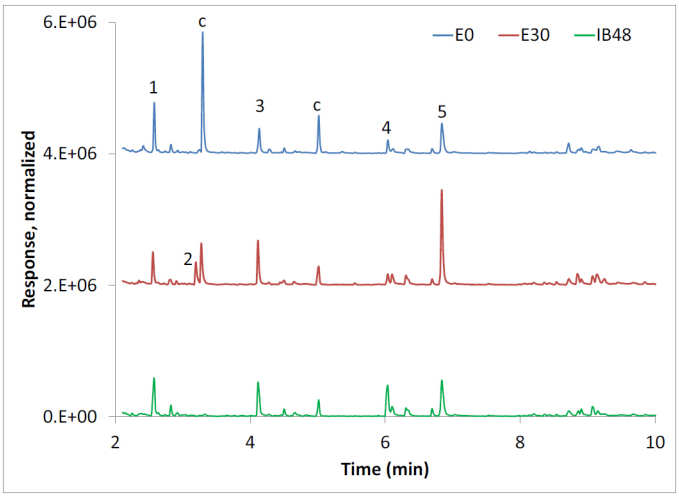

Figure 7. GC-MS trace of soot pyrolysis, showing the front part of the chromatogram. 1=benzene, 2=methyl propenoate, 3=toluene, 4=methyl ethenyl benzene, and 5=styrene. "c" indicates contaminant from the column.

To more easily examine the influence of fuel on the HC species, Figure 9 shows the response of several PAHs and the overall paraffin signal, normalized to 1 mg soot and the amount of gasoline in the fuel blend. The amount of individual PAHs is much higher for the E0, with the exception of pyrene. There appears to be an effect of fuel oxygen on the formation of PAHs during combustion. In previous mechanistic studies, ethanol is believed to interfere with the formation of aromatic compounds by short-circuiting the formation of conjugated double bonds [21],[22]. In addition, the paraffinic oil range compounds in the PM are higher for the alcohol fuels. This may indicate longer penetration length during injection and potential wall wetting resulting in the release of lubricant.

The predominance of PAHs in the HCs associated with GDI PM is a concern, particularly for the 5-7 ring PAHs. Benzo(a) pyrene has been listed by the International Agency for Research on Cancer (IARC) as a Class 1 carcinogen, “carcinogenic to humans” [23]. The other PAHs are typically listed as Class 2B or Class 3, “possibly carcinogenic to humans”, and “not classifiable as to its carcinogenicity to humans”. The presence of fuel oxygen appears to limit the formation of PAHs, which is positive. Previous studies have shown that gasoline PM has a higher PAH concentration than diesel PM, but diesel has traditionally dominated mobile source PM emissions. The major concern this study presents is that an increase in GDI vehicles in the fleet could potentially lead to more public exposure to gasoline PM than previously, and thus more exposure to PAHs associated with ultrafine particles.

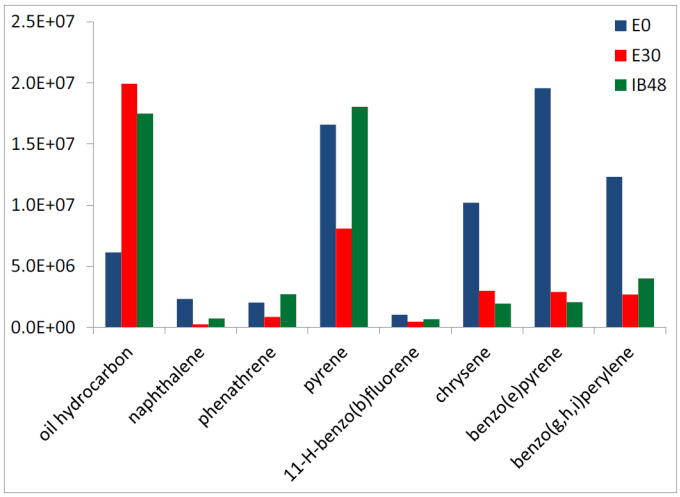

Figure 8. Relative amounts of selected HC species normalized for soot mass and fuel gasoline fraction. The oil hydrocarbon represents the total of all paraffinic species in the lubricant boiling range.

PM Sizing and Number Concentration

Size distributions (a minimum of six per fuel) were taken for all three fuels with the PMP and the averaged, dilution-corrected values are compared in Figure 11. Table 4 shows the brake specific particle number emissions in # of particles/kw·hr. The E0 emits the most particles which might be expected from the higher aromatic content and the highest mass concentration (Table 3.) The iBu48 falls in between E30 and E0 both in terms of particle numbers and peak particle size. The larger peak particle size for E30 is unexpected. In previous research, our laboratory determined that switching from E0 to E20 reduced peak particle size for steady state, stoichiometric operation at moderate load [5]. The rich operation may be the cause of the difference.

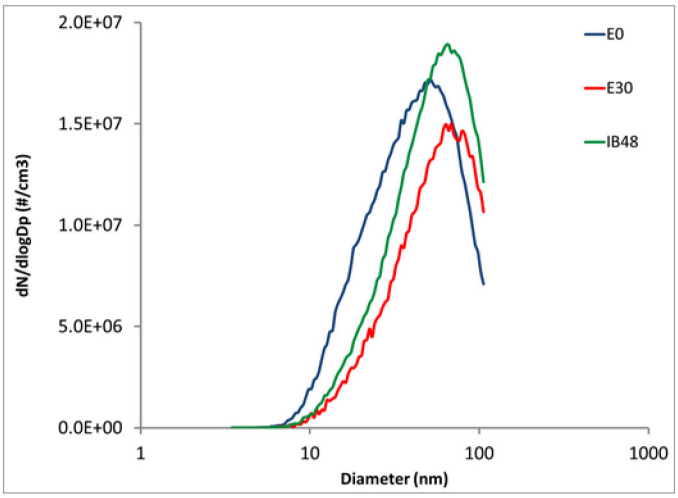

Figure 11. E0, E30, and iBu48 fuels particle size distributions.

Table 4. Brake specific particle number emissions and peak particle size for the three fuels.

Fuel	Total particle number emissions (#/kw.hr)	Geometric mean particle size (nm)
E0	2.82E+11	39.6
E30	1.93E+11	51.2
iBu48	2.42E+11	49.8

Aldehyde and Ketone Species

The aldehydes and ketones behaved as expected with the two alcohol blends emitting more of the corresponding aldehydes. E30 produced far more acetaldehyde, and iBu48 produced more C4 aldehydes. Similarly, the E0 produced the most formaldehyde, benzaldehyde, tolualdehyde, and dimethyl benzaldehyde. The latter three species are derivatives of the major gasoline compounds benzene, toluene, and xylenes. The results are shown in Figure 10. The inset shows the relatively large magnitude and variability of the acetaldehyde emissions from E30.

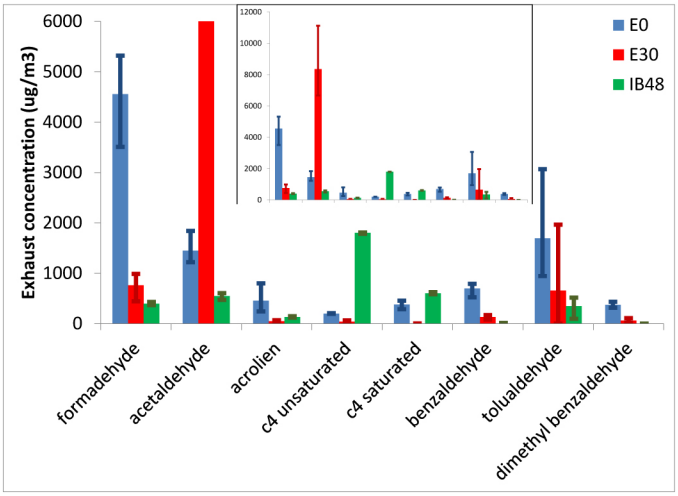

Figure 9. Average (n=3) aldehyde and ketone emissions for the three fuel blends. Range bars show the maximum and minimum values.

SUMMARY/CONCLUSIONS

A novel soot characterization method has been applied to PM from a GDI engine operating on gasoline and gasoline-alcohol blends. A rich air-fuel ratio and medium load were chosen to represent a vehicle acceleration condition, since we observed 10-20X more PM emissions during load transients. PAHs were the most abundant HC species in the PM, and fuel oxygenates appeared to suppress their formation. Rich operation, whether at cold start or during load changes, will likely remain the cause of the highest GDI emissions.

REFERENCES

1. Queiroz, C. and Tomanik, E., "Gasoline Direct Injection Engines - A Bibliographical Review," SAE Technical Paper 973113, 1997, doi:10.4271/973113.
2. Cole, R., Poola, R., and Sekar, R., "Exhaust Emissions of a Vehicle with a Gasoline Direct-Injection Engine," SAE Technical Paper 982605, 1998, doi:10.4271/982605.
3. Fraser, N., Blaxill, H., Lumsden, G., and Bassett, M., "Challenges for Increased Efficiency through Gasoline Engine Downsizing," *SAE Int. J. Engines* 2(1):991-1008, 2009, doi:10.4271/2009-01-1053.
4. Maricq, M. M., Podsiadlik, D. H., and Chase, R. E., "Examination of the Size-Resolved and Transient Nature of Motor Vehicle Particle Emissions," *Environ. Sci. Technol.*, vol. 33, no. 10, pp. 1618-1626, 1999, doi:10.1021/es9808806.
5. Storey, J., Barone, T., Norman, K., and Lewis, S., "Ethanol Blend Effects On Direct Injection Spark-Ignition Gasoline Vehicle Particulate Matter Emissions," *SAE Int. J. Fuels Lubr.* 3(2):650-659, 2010, doi:10.4271/2010-01-2129.
6. Storey, J., Barone, T., Thomas, J., and Huff, S., "Exhaust Particle Characterization for Lean and Stoichiometric DI Vehicles Operating on Ethanol-Gasoline Blends," SAE Technical Paper 2012-01-0437, 2012, doi:10.4271/2012-01-0437.
7. He, X., Ireland, J., Zigler, B., Ratcliff, M. et al., "The Impacts of Mid-level Biofuel Content in Gasoline on SIDI Engine-out and Tailpipe Particulate Matter Emissions," SAE Technical Paper 2010-01-2125, 2010, doi:10.4271/2010-01-2125.
8. Khalek, I., Bougher, T., and Jetter, J., "Particle Emissions from a 2009 Gasoline Direct Injection Engine Using Different Commercially Available Fuels," *SAE Int. J. Fuels Lubr.* 3(2):623-637, 2010, doi:10.4271/2010-01-2117.
9. Hedge, M., Weber, P., Gingrich, J., Alger, T. et al., "Effect of EGR on Particle Emissions from a GDI Engine," *SAE Int. J. Engines* 4(1):650-666, 2011, doi:10.4271/2011-01-0636.
10. Maricq, M. M., Podsiadlik, D. H., and Chase, R. E., "Gasoline vehicle particle size distributions: Comparison of steady state, FTP, and US06 measurements," *Environ. Sci. Technol.*, vol. 33, no. 12, pp. 2007-2015, Jun. 1999, doi:10.1021/es981005n.
11. Zhang, S. and McMahon, W., "Particulate Emissions for LEV II Light-Duty Gasoline Direct Injection Vehicles," *SAE Int. J. Fuels Lubr.* 5(2):637-646, 2012, doi:10.4271/2012-01-0442.
12. U.S. Environmental Protection Agency, "Partial Grant of Clean Air Act Waiver Application Submitted by Growth Energy to Increase the Allowable Ethanol Content of Gasoline to 15 percent; Decision of the Administrator," vol. 76, no. 17, pp. 4662-4683.
13. Jung, H., Shelby, M., Newman, C., and Stein, R., "Effect of Ethanol on Part Load Thermal Efficiency and CO2 Emissions of SI Engines," *SAE Int. J. Engines* 6(1):456-469, 2013, doi:10.4271/2013-01-1634.
14. Szybist, J. P., Youngquist, A. D., Barone, T. L., Storey, J. M., Moore, W. R., Foster, M., and Confer, K., "Ethanol Blends and Engine Operating Strategy Effects on Light-Duty Spark-Ignition Engine Particle Emissions," *Energy & Fuels*, vol. 25, pp. 4977-4985, 2011, doi:10.1021/ef201127y.
15. Moore, W., Foster, M., and Hoyer, K., "Engine Efficiency Improvements Enabled by Ethanol Fuel Blends in a GDi VVA Flex Fuel Engine," SAE Technical Paper 2011-01-0900, 2011, doi:10.4271/2011-01-0900.
16. Strzelec, A., Toops, T. J., and Daw, C. S., "Oxygen Reactivity of Devolatilized Diesel Engine Particulates from Conventional and Biodiesel Fuels," *Energy & Fuels*, vol. 27, no. 7, pp. 3944-3951, Jul. 2013, doi:10.1021/ef400440a.
17. Abdul-Khalek, I., Kittelson, D., Graskow, B., Wei, Q. et al., "Diesel Exhaust Particle Size: Measurement Issues and Trends," SAE Technical Paper 980525, 1998, doi:10.4271/980525.
18. Giechaskiel, B., Dilara, P., and Sandbach, E, Andersson, J., "Particle measurement programme (PMP) light-duty inter-laboratory exercise: comparison of different particle number measurement systems," *Meas. Sci. Technol.*, vol. 19, no. 9, 2008, doi:10.1088/0957-0233/19/9/095401.
19. "Regulation No 83 of the Economic Commission for Europe of the United Nations (UN/ECE) - Uniform provisions concerning the approval of vehicles with regard to the emission of pollutants according to engine fuel requirements," *Off. J. Eur. Union*, vol. 15.2.2012, 2012.
20. Birch, M. E., and Cary, R. a., "Elemental Carbon-Based Method for Monitoring Occupational Exposures to Particulate Diesel Exhaust," *Aerosol Sci. Technol.*, vol. 25, no. 3, pp. 221-241, Jan. 1996, doi:10.1080/02786829608965393.
21. Litzinger, T., Wu, J., and Santoro, R., "Reduction of PAH and soot in premixed ethylene-air flames by addition of ethanol," *Combust. Flame*, vol. 144, p. 675, 2006, doi:10.1016/j.combustflame.2006.06.006.
22. Buchholz, B., Cheng, A., and Dibble, R., "Isotopic Tracing of Bio-Derived Carbon from Ethanol-in-Diesel Blends in the Emissions of a Diesel Engine," SAE Technical Paper 2002-01-1704, 2002, doi:10.4271/2002-01-1704.
23. "IARC Monographs on the Evaluation of Carcinogenic Risk to Humans," International Agency for Research on Cancer, 2013. Available: http://monographs.iarc.fr/ENG/Classification/.

CONTACT INFORMATION

John M. E. Storey
Oak Ridge National Laboratory
P.O. Box 2008
MS 6472
Oak Ridge
TN 37830
phone: 865-946-1232
fax:865-946-1354
storeyjm@ornl.gov

ACKNOWLEDGMENTS

This work was supported by the U.S. Department of Energy (DOE), Vehicle Technologies Office, Fuels Technology activity. The authors gratefully acknowledge the support and guidance of Kevin Stork, and Steve Przesmitski at DOE. The authors wish to thank Mr. Steve Whitted for his technical support and guidance on hardware installation.

DEFINITIONS/ABBREVIATIONS

A/F - air fuel ratio

ASTM - American Society for Testing and Materials

AKI - anti-knock index

BMEP - brake mean effective pressure

CA bTDC - crank angle before top dead center

CPC - Condensation Particle Counter

DISI - direct injection spark ignition

DMA - Differential Mobility Analyzer

DNPH - dinitro-phenylhyrdrazine

DVPE - dry vapor pressure equivalent

E0 - 100% gasoline

E30 - 30% ethanol in gasoline

EC - elemental carbon

ESI-MS - electrospray ionization mass spectrometry

EtOH - ethanol

GC - gas chromatograph

GDI - gasoline direct injection

HC - hydrocarbon

HPLC - high performance liquid chromatography

iBu48 - 48% isobutanol in gasoline

LHV - lower heating value

OC - organic carbon

PAH - polycyclic aromatic hydrocarbons

PFI - port fuel injected

PM - particulate matter

PMP - Particulate Matter Programme

PTFE - polytetrafluoroethylene

RPM - repetitions per minute

SG - specific gravity

SMPS - Scanning Mobility Particle Sizer

TDP-GC-MS - Thermal desorption/pyrolysis-gas chromatography-mass spectroscopy